HHS Public Access

Author manuscript

Phytochemistry. Author manuscript; available in PMC 2019 February 01.

Published in final edited form as:

Phytochemistry. 2018 February ; 146: 36–46. doi:10.1016/j.phytochem.2017.11.010.

The Natural Sesquiterpene Lactones Arglabin, Grosheimin, Agracin, Parthenolide, and Estafiatin Inhibit T Cell Receptor (TCR) Activation

Igor A. Schepetkin[1], **Liliya N. Kirpotina**[1], **Pete T. Mitchell**[1], **Anarkul S. Kishkentaeva**[2], **Zhanar R. Shaimerdenova**[2], **Gayane A. Atazhanova**[2], **Sergazy M. Adekenov**[2], and **Mark T. Quinn**[1]

[1]Department of Microbiology and Immunology, Montana State University, Bozeman, MT 59717, United States

[2]International Research and Production Holding “Phytochemistry”, Karaganda 100009, Republic of Kazakhstan

Abstract

Inhibition of the T cell receptor (TCR) pathway represents an effective strategy for the treatment of T cell-mediated inflammatory and autoimmune diseases. To identify natural compounds that could inhibit inflammatory T cell responses, we screened 13 sesquiterpene lactones, including achillin, arglabin, argolide, argracin, 3β-hydroxyarhalin, artesin, artemisinin, estafiatin, grosheimin, grossmisin, leucomisine, parthenolide, and taurine, for their ability to modulate activation-induced Ca^{2+} mobilization in Jurkat T cells. Five of the compounds (arglabin, grosheimin, argracin, parthenolide, and estafiatin) inhibited anti-CD3-induced mobilization of intercellular Ca^{2+} ($[Ca^{2+}]_i$) in Jurkat cells, with the most potent being parthenolide and argacin (IC_{50} = 5.6 and 6.1 μM, respectively). Likewise, phosphorylation of extracellular signal-regulated kinase (ERK) 1/2 in activated Jurkat cells was inhibited by these five compounds, with the most potent being parthenolide and estafiatin (IC_{50} = 13.8 and 15.4 μM, respectively). These compounds also inhibited ERK1/2 phosphorylation in primary human T cells and depleted intracellular glutathione. In contrast, none of the sesquiterpene lactones inhibited ERK1/2 phosphorylation in HL60 cells transfected with *N*-formyl peptide receptor 2 (FPR2) and stimulated with the FPR2 peptide agonist WKYMVM, indicating specificity for T cell activation. Estafiatin, a representative sesquiterpene lactone, was also profiled in a cell-based phosphokinase array for 43 kinase phosphorylation sites, as well as in a cell-free competition binding assay for its ability to compete with an active-site directed ligand for 95 different protein kinases. Besides inhibition of ERK1/2 phosphorylation, estafiatin also inhibited phosphorylation of p53, AMPKα1, CREB, and p27 elicited by TCR activation in Jurkat cells, but it did not bind to any of 95 kinases

Address for Correspondence: Mark T Quinn, Ph.D., Department of Microbiology and Immunology, Montana State University, Bozeman, MT 59717, Phone: 1-406-994-4707, Fax: 1-406-994-4303, mquinn@montana.edu.

Conflict of Interest

The authors have declared that there is no conflict of interest.

evaluated. These results suggest that arglabin, grosheimin, agracin, parthenolide, and estafiatin can selectively inhibit initial phases of TCR activation and may be natural compounds with previously undescribed immunotherapeutic properties.

Graphical Abstract

T cell activation is suppressed by sesquiterpene lactones containing an α-methylene-γ-lactone backbone, as demonstrated by the inhibition of Ca2+ mobilization, ERK1/2 phosphorylation, and GSH depletion.

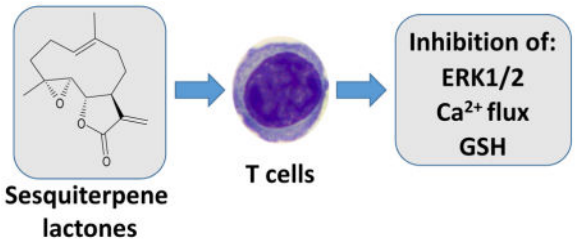

Keywords

Sesquiterpene lactones; Jurkat T cells; T cell receptor; kinase; phosphorylation; calcium flux; glutathione

1. Introduction

Sesquiterpene lactones are natural products that are abundant in plants of the Asteraceae family and possess a broad spectrum of biological activities, including anticancer, antibacterial, antifungal, anti-inflammatory, and immunomodulatory activities [reviewed in (Chadwick et al., 2013; Hou and Huang, 2016; Ren et al., 2016)]. Although the anticancer and anti-proliferative activities of various sesquiterpene lactones and their synthetic derivatives are well known, and some sesquiterpene lactones are currently under clinical evaluation [reviewed in (Ren et al., 2016)], the molecular mechanisms involved in their anti-inflammatory and T cell immunomodulatory activities have not been clearly elucidated. For example, parthenolide has been found to inhibit p65 NF-κB binding to DNA and IκB-kinase activity in Jurkat T cells (Garcia-Pineres et al., 2001; Garcia-Pineres et al., 2004) and cytokine production in anti-CD3/CD28-stimulated peripheral blood T cells from allergic and normal donors (Li-Weber et al., 2002). However, it is still not clear if sesquiterpene lactones can alter other pathways during T cell activation.

T cells are essential for inflammation and adaptive immune responses, and deregulation of T cell function can contribute to autoimmune diseases [e.g., see (Sauer et al., 2015)]. The TCR recognizes and responds to antigenic peptides in the context of major histocompatibility complex (MHC)-encoded molecules. Upon MHC-peptide engagement, TCR components (associated with CD3 chains) initiate Ca^{2+} mobilization and mitogen-activated protein kinase (MAPK) phosphorylation cascades, including extracellular signal-regulated kinase (ERK) activation, which trigger multiple signaling pathways (Koike et al., 2003). Thus, specific inhibitors of TCR signaling represent potential therapeutics for treating autoimmune

diseases, and the identification of such compounds has been of significant interest [e.g., see (Visperas et al., 2017)]. Analysis of public microarray repositories predicts that TCR signaling may be involved in the effects of parthenolide and artemisinin on acute myelogenous leukemia (Engreitz et al., 2010; Huang et al., 2013). Indeed, SM905, a synthetic artemisinin derivative, was found to inhibit TCR-mediated T cell proliferation and MAPK phosphorylation (Wang et al., 2007). Another artemisinin analogue, SM934, was recently found to attenuate collagen-induced arthritis by suppressing T follicular helper cells and T helper 17 (Th17) cells (Lin et al., 2016). Similarly, parthenolide inhibited the initiation of experimental autoimmune neuritis by decreasing Th1 and Th17 cells (Zhang et al., 2017). However, molecular mechanisms involved in the regulation of T cell activity by sesquiterpene lactones are still not well defined. For example, the effects of sesquiterpene lactones on T cell Ca^{2+} mobilization and ERK phosphorylation following TCR stimulation have not been previously assessed.

Here, we studied the capacity of 13 plant-derived sesquiterpene lactones to inhibit initial phases of TCR activation and showed that five of these natural sesquiterpene lactones (arglabin, parthenolide, grosheimin, agracin, and estafiatin) inhibited Ca^{2+} mobilization and ERK1/2 phosphorylation induced by TCR activation. Thus, our studies demonstrate that these sesquiterpene lactones can selectively inhibit initial phases of TCR activation.

2. Results

2.1. Effect of sesquiterpene lactones on lymphocyte Ca^{2+} mobilization

TCR activation results in rapid mobilization of intracellular Ca^{2+}, which represents one of the early signaling events that can be monitored in lymphocyte activation (Ishikawa et al., 2003). Thus, we evaluated the effect of a variety of natural sesquiterpene lactones on Ca^{2+} mobilization induced by anti-CD3 antibodies in Jurkat T cells (Table 1). The set of 13 natural sesquiterpene lactones tested was assembled to maximize chemical diversity and included compounds with germacranolide (compounds **3**, **4**, and **12**), eudesmane (compounds **5**, **7**, and **13**), guaianolide (compounds **1, 2**, **8**, **9**, **10**, and **11**), and cadinanolide (compound **6**) structures. Six of the germacranolide and eudesmane compounds contain an α-methylene-γ-lactone ring, two of guaianolide and germacranolide compounds have an epoxide group, and one contains an endoperoxide bridge. As shown in Figure 1A, the intracellular Ca^{2+} flux rapidly induced after Jurkat cell activation was significantly inhibited by pretreatment of these cells with estafiatin and parthenolide. Likewise, arglabin, agracin, and grosheimin also dose-dependently inhibited Jurkat T cell activation-induced intracellular Ca^{2+} flux, and a representative dose–response curve for inhibition of Jurkat cell Ca^{2+} mobilization by agracin is shown in Figure 1B. In contrast, the other 8 sesquiterpene lactones tested had no effect on this response (Table 2).

All five active sesquiterpene lactones contain an α-methylene-γ-lactone ring, which may react with nucleophiles, such as cysteine sulfhydryl group(s) of glutathione (GSH), redox-sensitive kinases and other enzymes, by a Michael-type addition (Butturini et al., 2013; Visperas et al., 2015). To evaluate whether a redox-event is important in modulation of TCR activation by these compounds, Jurkat cells were pretreated for 3 h at 37 °C with 5 mM glutathione ethylene ester (GEE), a cell-permeable GSH (Butturini et al., 2013), and

thereafter for 20 min with different concentrations of agracin and parthenolide, the most potent inhibitors of TCR activation-induced Ca^{2+} flux (see Table 2). Interestingly, we found that pretreatment with GEE reversed much of the inhibitory effect of parthenolide (not shown) and agracin on intracellular Ca^{2+} mobilization (Figure 1B). Note, however, that the highest concentrations of lactone could partially overcome these effects of GEE (Figure 1B).

Thapsigargin, a sesquiterpene lactone from *Thapsia garganica*, is an inhibitor of the sarco/endoplasmic reticulum Ca^{2+} ATPase (SERCA) and raises intracellular Ca^{2+} by blocking the ability of the cell to pump Ca^{2+} into the sarcoplasmic and endoplasmic reticula (Rogers et al., 1995). Thus, we evaluated the direct effect of our selection of sesquiterpene lactones on Ca^{2+} flux in Jurkat T cells compared to thapsigargin. While we confirmed that thapsigargin could stimulate $[Ca^{2+}]_i$ accumulation in Jurkat cells, none of the 13 sesquiterpene lactones tested increased $[Ca^{2+}]_i$ in these cells. As examples, the direct effects of thapsigargin, estafiatin, and artemisinin on Jurkat T cell Ca^{2+} levels are shown in Figure 2.

To test cell specificity of the sesquiterpene lactones on Ca^{2+} flux, we also evaluated if they modulated Ca^{2+} mobilization in activated human neutrophils and HL60 cells transfected with FPR1 and FPR2. None of sesquiterpene lactones directly stimulated Ca^{2+} mobilization in neutrophils or transfected HL60 cells (data not shown). Likewise, treatment of these cells with various concentrations of sesquiterpene lactones for 20 min and had no effect on Ca^{2+} mobilization induced by FPR1/FPR2 agonists (*f*MLF in neutrophils and FPR1-HL60 cells or WKYMVM in FPR2-HL60 cells) (Table 2), indicating that the inhibitory effect was specific for TCR activation.

Considering the apparent selectivity of sesquiterpene lactones towards inhibition of Ca^{2+} flux in Jurkat T cells, we evaluated if N-ethylmaleimide (NEM), a highly reactive but nonspecific cysteine alkylating reagent, would also inhibit lymphocyte activation similarly to the sesquiterpene lactones. However, we found that pretreatment with NEM led to a dose-dependent inhibition of Ca^{2+} flux in all cells tested, with IC_{50} values in nanomolar range. Indeed, NEM pretreatment inhibited Ca^{2+} flux in Jurkat cells stimulated with anti-CD3/CD28 (IC_{50} = 175 ± 70 nM) and in FPR1-HL60 cells (IC_{50} = 360 ± 34 nM) or human neutrophils (IC_{50} = 860 ± 330 nM) stimulated with 5 nM *f*MLF. Thus, comparison of the observed effects of NEM and sesquiterpene lactones in lymphoid and myeloid cells supports the conclusion that these sesquiterpene lactones modulate a specific target or targets in lymphocytes rather than nonspecifically modifying cysteines in any cell type.

2.2. Effect of estafiatin on protein kinase activity

Stimulation of the TCR in Jurkat cells activates multiple signaling pathways, including a variety of protein kinases (Kim and White, 2006; Koike et al., 2003). To evaluate the effect of sesquiterpene lactones on protein kinase signaling, we selected estafiatin as a representative compound, as it contains both α-methylene-γ-lactone and epoxide moieties (see Table 1). To simultaneously evaluate effects of estafiatin on phosphorylation of various kinases and their substrates, we utilized a human phospho-kinase array Proteome Profiler, which monitors the phosphorylation of 43 kinase phosphorylation sites (see list of kinases in the *Experimental* section). While estafiatin itself did not increase phosphorylation of the arrayed kinases (Figure 3A), treatment with anti-CD3/CD28 significantly increased

phosphorylation of ERK1/2 [phosphorylation sites Thr202/Tyr204, Thr185/Tyr187; fold increase (FI) = 6.7], AMPKα1 (Thr183; FI=2.4), CREB (Ser133; FI=4.7), p53 (S392; FI=2.2), and p27 (Thr180/Tyr182; FI= 7.3) in Jurkat cells (Figure 3B, grey bars). Importantly, pretreatment of Jurkat cells with estafiatin (50 μM) for 20 min at 37 °C completely inhibited the TCR activation-induced phosphorylation of ERK1/2, p53, AMPKα1, CREB, and p27 (Figure 3C).

The suppression of ERK1/2 phosphorylation might result from direct inhibition or inhibition of other upstream kinase(s). Thus, we evaluated the direct binding activity of estafiatin against a panel of 95 protein kinases representing all known kinase families in a cell-free competition binding assay for the ability of estafiatin to compete with binding of an active-site directed ligand (DiscoveRx KINOMEscan). However, estafiatin did not bind directly to any of the kinases tested (data not shown), including zeta-chain-associated protein kinase 70 kDa (ZAP70), Fyn oncogene, spleen tyrosine kinase (Syk), lymphocyte-specific protein tyrosine kinase (Lck), liver kinase B1 (LKB1), ERK1, and ERK2. Thus, estafiatin likely modulates kinase activity through alternative mechanisms. For example, one possibility to be evaluated in future studies is that estafiatin could prevent thiol-sensitive tandem-SH2 domains of ZAP-70 and Syk from binding to phosphorylated ITAMs [see (Visperas et al., 2017; Visperas et al., 2015)].

ERK1/2 phosphorylation was one of the main TCR activation-induced responses observed in our kinase array (Figure 3B) [also see (Kim and White, 2006)]. Thus we further characterized this response and its modulation by the active sesquiterpene lactones. Although none of compounds directly stimulated ERK1/2 phosphorylation (data not shown), pretreatment of Jurkat T cells with various concentrations of these compounds, followed by activation with anti-CD3/CD28 antibodies showed that the five compounds that inhibited Ca^{2+} mobilization (arglabin, agracin, estafiatin, grosheimin, and parthenolide) also significantly inhibited TCR activation-induced ERK1/2 phosphorylation in a dose-dependent manner, with IC_{50} values in the micromolar range (Table 2). As examples, dose-dependent inhibition of ERK1/2 phosphorylation by parthenolide and estafiatin are shown in Figure 4. Likewise, pretreatment of human primary T cells with parthenolide or estafiatin also suppressed ERK1/2 phosphorylation stimulated by anti-CD3/CD28 antibodies (Figure 5), verifying that this effect was relevant to primary cells. Finally, pretreatment of Jurkat cells with GEE reversed the inhibitory effect of parthenolide and estafiatin on ERK1/2 phosphorylation (Figure 4), indicating that restoring $[GSH]_i$ could overcome at least some of the inhibitory effects of these sesquiterpene lactones.

To evaluate target specificity of the effect on ERK1/2 phosphorylation activated through the TCR, we also evaluated if the sesquiterpene lactones could inhibit ERK1/2 phosphorylation stimulated by other receptors. For example, activation of FPR2 is known to induce ERK1/2 phosphorylation (Schepetkin et al., 2014). Thus, we pretreated FPR2-HL60 cells with various concentrations of the sesquiterpene lactones (up to 50 μM), and the cells were activated with 5 nM WKYMVM, a peptide FPR2 agonist. However, none of the compounds tested inhibited FPR2-dependent ERK1/2 phosphorylation (Table 2), suggesting again that sesquiterpene lactones specifically inhibit TCR-dependent activation.

2.3. GSH reactivity of the sesquiterpene lactones

GSH is an important regulator of cellular redox equilibrium. The TCR-mediated response is very sensitive to changes in intercellular GSH levels ($[GSH]_i$) (Gringhuis et al., 2002), and some sesquiterpene lactones can decrease $[GSH]_i$ in various human cells by reacting with cysteine (Itoh et al., 2009; Scarponi et al., 2014). Thus, we evaluated if the selected sesquiterpene lactones can react with GSH in Jurkat T cells. Screening of sesquiterpene lactone reactivity with cytosolic GSH showed that the compounds that inhibited Ca^{2+} mobilization and ERK1/2 phosphorylation also depleted $[GSH]_i$ in Jurkat cells, with the most potent being argracin and parthenolide (Table 2), and a representative concentration-dependent decrease of $[GSH]_i$ in Jurkat T cells after argracin treatment is shown in Figure 6.

2.4. Effect of sesquiterpene lactones on anti-CD3 binding

As described above, sesquiterpene lactones can alkylate thiol groups on biological macromolecules, including cysteine residues of target proteins (Garcia-Pineres et al., 2001; Lagoutte et al., 2016; Wagner et al., 2006; Zhang et al., 2015). Although the highly conserved membrane-proximal tetracysteine motif in the stalk region of CD3 is not required for CD3 dimerization, modification of these cysteine residues has been reported to reduce assembly of CD3δε with TCRα (Xu et al., 2006). Thus, we evaluated if the active sesquiterpene lactones could affect the ability of anti-CD3 monoclonal antibodies to bind the extracellular region of CD3. Although pretreatment with anti-CD3 antibody (5 μg/ml) itself completely blocked the binding of fluorescent anti-CD3 antibody to Jurkat cells, neither arglabin, grosheimin, agracin, parthenolide, or estafiatin (all tested at 50 μM for 20 min at 37 °C) reduced binding of APC-labeled anti-CD3 antibody to the extracellular region of CD3 (data not shown).

2.5. Effect of sesquiterpene lactones on cell toxicity

To ensure that the results were not influenced by possible compound toxicity, cytotoxicity of the sesquiterpene lactones was evaluated at various concentrations up to 50 μM in Jurkat and isolated T cells during a 30 min incubation with the compounds. None of the sesquiterpene lactones affected cell viability at the highest tested concentrations (Table 2 for Jurkat T cells and data not shown for primary human T cells), thereby verifying that these compounds were not cytotoxic during the 30 min incubation period of our assays.

3. Discussion

Plant-derived sesquiterpene lactones exhibit a broad spectrum of pharmacological properties, including immunomodulation and anti-inflammatory activity (reviewed in (Chadwick et al., 2013; Hou and Huang, 2016; Ren et al., 2016)). For example, the therapeutic potential of arglabin and its chemical derivatives was recently reviewed (Adekenov, 2016). Parthenolide was previously studied regarding inhibition of NF-κB activation and cytokine production in Jurkat and primary T cells (Garcia-Pineres et al., 2001; Garcia-Pineres et al., 2004; Li-Weber et al., 2002). Although several sesquiterpenes have been reported to inhibit ERK phosphorylation in different cell lines and macrophages (D'Anneo et al., 2013; Saadane et al., 2011; Wang et al., 2011; Ye et al., 2015), their effects on Ca^{2+} mobilization and ERK phosphorylation following TCR stimulation have not been

previously assessed. In the present study, we evaluated the immunomodulatory effects of 13 natural sesquiterpene lactones and found that five of the tested compounds (arglabin, argracin, estafiatin, grosheimin, and parthenolide) specifically inhibited early phases of TCR activation but had no effect on phagocyte activation through FPR1/2. Activation of Jurkat T and primary T cells was suppressed by these sesquiterpene lactones, as demonstrated by inhibition of Ca^{2+} mobilization and ERK1/2 phosphorylation. These lactones also depleted $[GSH]_i$ in Jurkat T cells. Although several naturally occurring compounds, including parthenolide, have been previously reported to modulate T cell activity stimulated through the TCR (Garcia-Pineres et al., 2001; Garcia-Pineres et al., 2004; Li-Weber et al., 2002; Liu et al., 2011), this is the first report demonstrating inhibition of TCR activation-induced Ca^{2+} mobilization and ERK1/2 phosphorylation by natural sesquiterpene lactones.

Among of the sesquiterpene lactones evaluated, only parthenolide and artemisinin have been studied previously for their effects on ERK phosphorylation, but in different cells (D'Anneo et al., 2013; Saadane et al., 2011; Wang et al., 2011). For example, ERK1/2 phosphorylation was inhibited by parthenolide in cystic fibrosis cell cultures (Saadane et al., 2011) and murine osteoclast precursors (Kim et al., 2014). However, parthenolide activated ERK1/2 phosphorylation in human osteosarcoma MG63 and melanoma SK-MEL-28 cells (D'Anneo et al., 2013). Although artemisinin can suppress ERK1/2 phosphorylation in THP-1 macrophages (Wang et al., 2011), we did not observe inhibition of ERK1/2 phosphorylation by this compound in Jurkat T cells (Table 2). It should be noted that there has been no reported correlation between $[GSH]_i$ depletion by various natural compounds and ERK activity. For example, the diterpenoid oridonin, which also contains an α-methylene-γ-lactone ring, reduced $[GSH]_i$ in hepatic stellate HSC-T6 cells but also induced ERK1/2 phosphorylation (Kuo et al., 2014). Together, these data indicate the effects of sesquiterpene lactones are cell-specific but may also depend on how various agonists engage downstream signaling pathways.

The precise target of the active sesquiterpene lactones identified here is currently not known, although it is known that the α-methylene-γ-lactone group is important for their biological activity. For example, previous structure–activity relationship analysis showed that the α-methylene-γ-lactone ring was the site of attack of the cysteine residues on GSH, various receptors, protein kinases, and transcription factor subunits (Garcia-Pineres et al., 2001; Lagoutte et al., 2016; Wagner et al., 2006; Zhang et al., 2015). Indeed, all five active sesquiterpene lactones that inhibited Ca^{2+} flux, blocked ERK1/2 phosphorylation, and depleted $[GSH]_i$ in Jurkat T cells contain an α-methylene-γ-lactone ring, whereas only one compound with an α-methylene-γ-lactone ring (argolide) was inactive (Tables 1 and 2). Note, however, that parthenolide, the most potent compound in both the Ca^{2+} flux and ERK1/2 assays, also possesses an epoxide group. Thus, we cannot exclude the possibility that inhibitory effect on TCR activation is greater when a sesquiterpene lactone has two potentially reactive centers that could react with biological nucleophiles, such as sulfhydryl groups. Artemisinin also has a reactive endoperoxide bridge. However, this compound was inactive in all of our assays, indicating that the endoperoxide functionality and/or formation of free radicals via cleavage of the endoperoxide bond does not play an important role in modulation of TCR activity or that the geometry of this molecule is not suitable for interaction with the relevant molecular targets. Thus, based on the direct correlation between

biological activity and number of chemically reactive α-methylene-γ-lactone/epoxide groups in the compounds possessing very similar molecular structure, we suggest that modulating influence of the other structural factors on bioactivity is lower.

Recently, it was reported that GSH is dispensable for initial T cell activation (Mak et al., 2017). However, sesquiterpene lactones likely can act on several thiol-sensitive targets, and concurrent GSH depletion would increase the aggregate effect of these compounds on T cell activation. Following depletion of $[GSH]_i$, the major anti-oxidant molecule and redox-buffer in cells, the active sesquiterpene lactones could then induce oxidative stress and/or form protein adducts (Carlisi et al., 2016). Indeed, regulation of protein kinase activity can occur via several redox-cycles involving thioredoxin, GSH-dependent enzymes, and reactive oxygen species (ROS). For example, apoptosis signal-regulating kinase 1 (ASK1) is physically associated with thioredoxin, making thioredoxin a redox-sensitive physiological regulator of ASK1 activity and ASK1-associated MAPK (Davis et al., 2001). Likewise, glutathione S-transferase P1-1 (GSTP) can interact with JNK, and this protein-protein interaction can sequester JNK and act as a regulator of this MAPK (Tew and Townsend, 2011). ROS-induced cysteine oxidation in proteins involves initial formation of sulfenic acid, which can subsequently react with GSH to form S-glutathionylated proteins (Reddie and Carroll, 2008), and the importance of these specific oxidative cysteine modifications in direct regulation of tyrosine kinases was recently described (Heppner et al., 2016). Because the inhibition of Ca^{2+} mobilization and ERK1/2 phosphorylation were significantly diminished when Jurkat cells were incubated with GEE, S-glutathionylation of protein kinases engaged in TCR activation is likely to be triggered by increased oxidative stress induced by the decrease in cellular GSH.

It should be noted that the α-methylene-γ-lactone ring of sesquiterpene lactones plays a critical role in mediating cytotoxicity via GSH depletion (Kupchan et al., 1971; Carlisi et al., 2015), as GSH depletion can activate apoptotic caspases with subsequent cell death (Lee et al., 2013; Khan et al., 2013). In the present studies, we investigated very early events in T cell activation (first 30 min) when no cytotoxicity was observed. Thus, assessment of the relationship between structure of the natural compounds and their cytotoxicity profile during long-term treatment (hours and days) and with a variety of immune cells will be important to evaluate in future studies.

Sesquiterpene lactones can also directly react with proteins. For example, parthenolide reacts with albumin cysteine residues exclusively via its α-methylene-γ-lactone moiety, while the epoxide structure is not involved in the reaction (Ploger et al., 2015). Thus, it is clearly feasible that our active sesquiterpene lactones could form adducts with macromolecules engaged in TCR-dependent activation. Upon TCR stimulation, tyrosine kinases Fyn and Lck phosphorylate ITAMs in the TCR, which recruit tyrosine kinases Syk and ZAP70 to phosphorylate the linker of activated T cells (LAT), resulting in the formation of a complex consisting of various components, including interleukin-2-inducible tyrosine kinase (Itk) and phospholipase C (PLC) γ1 (Fu et al., 2010; Zhang et al., 1998). Activated PLCγ1 hydrolyzes phosphatidylinositol 4,5-bisphosphate to generate inositol 1,4,5-trisphosphate (IP3), which stimulates the release of Ca^{2+} from intracellular stores. Ca^{2+} mobilization leading to activation of multiple pathways, including ERK1/2, which

eventually activate specific nuclear factors (Winslow et al., 2003). Using a high-throughput screen, Visperas et al. (Visperas et al., 2017; Visperas et al., 2015) recently identified several small-molecule compounds that covalently react with cysteine residues of the ZAP70 tandem SH2 module and inhibit its binding to a phosphorylated ITAM-derived peptide. Thus, based on the reactivity of the active sesquiterpene lactones for cysteine, it is possible that they can similarly induce redox-dependent post-translational modification of cysteine residues in the ZAP70 SH2 module to regulate its function, and this is currently being evaluated. Another possibility is that the active sesquiterpene lactones interact with NEM-sensitive fusion protein (NSF), soluble NEM-sensitive factor attachment protein receptor (SNARE) proteins, or tubulin and/or dynein systems, which play important roles in forming signaling clusters upon TCR activation (Heller et al., 2001; Larghi et al., 2013; Philipsen et al., 2013). Indeed, recent high-content screening identified parthenolide as an inhibitor of cytoplasmic dynein-mediated transport and microtubule formation and suggested it may react with detyrosinated tubulin (Johnston et al., 2012; Miyata et al., 2008; Whipple et al., 2013). Whether the other active sesquiterpene lactones identified here can also inhibit these pathways in T cells will need to be investigated in future studies.

Thapsigargin, a sesquiterpene lactone and potent inhibitor of SERCA activity, induces Ca^{2+} release from the endoplasmic reticulum and the subsequent opening of plasma membrane-specific Ca^{2+} channels responsible for the store-operated calcium entry (Cerveira et al., 2015). Consistent with these observations, we found that thapsigargin stimulated Ca^{2+} accumulation in Jurkat T cells. Although artemisinin inhibited SERCA activity in *Plasmodium falciparum* (Eckstein-Ludwig et al., 2003), none of the test compounds, including artemisinin, induced Ca^{2+} flux in human neutrophils, Jurkat T cells, or FPR1/2 transfected HL60 cells. Based on these data, we conclude that the active sesquiterpene lactones do not inhibit SERCA in these cells.

Analysis of estafiatin, a representative active sesquiterpene lactone with α-methylene-γ-lactone and epoxide moieties, showed that this compound inhibited AMPKα1 phosphorylation but did not bind with LKB1, a main kinase that phosphorylates AMPKα1. Because estafiatin also does not bind kinase modules of ZAP70, Fyn, Syk, and Lck, which are the most proximal kinases to be activated downstream of the TCR (Lovatt et al., 2006), it could be possible that the active sesquiterpene lactones may directly interact with an extracellular region of CD3 and prevent activation of the TCR complex by anti-CD3. On the other hand, we also found that all of the active sesquiterpene lactones did not affect anti-CD3 binding with extracellular region of CD3 on Jurkat T cells, so such an interaction would have to involve a different region of the molecule than that targeted by anti-CD3.

Our results show that the nonselective thiol-modifying reagent NEM is a potent inhibitor of Ca^{2+} flux initiated via TCR activation in Jurkat cells, as well as FPR1 stimulation in FPR1-HL60 cells and neutrophils stimulated by *f*MLF, as reported previously (Hsu et al., 2005). Given that the active sesquiterpene lactones did not inhibit Ca^{2+} mobilization in activated FPR1-HL60 cells and neutrophils, we conclude that these compounds are clearly more selective than NEM. Upon specific ligand binding and activation of FPR, intracellular domains of FPR mediate signaling to G-proteins, which trigger several agonist-dependent signal transduction pathways, including Ca^{2+} mobilization and ERK1/2 phosphorylation

(Cattaneo et al., 2013; Gripentrog and Miettinen, 2008). Although intact thiol groups are important for FPR ligand binding (Lane and Lamkin, 1982), the sesquiterpene lactones tested apparently did not block binding of FPR1/2 with specific ligands since no effect on activation was observed. Likewise, these compounds did not appear to interfere with the PLC/IP3 pathway in these cells, suggesting that their molecular target(s) could be located upstream.

In conclusion, our experimental studies demonstrate that arglabin, argracin, estafiatin, grosheimin, and parthenolide can interact with pathways involved in initial phases of TCR activation, resulting in inhibition of this response. All five active sesquiterpene lactones that inhibited Ca^{2+} mobilization, blocked ERK1/2 phosphorylation, and depleted $[GSH]_i$ in Jurkat T cells contained an α-methylene-γ-lactone ring, indicating an important role for this structure in compound bioactivity. Overall, these results suggest a potential new strategy for developing novel medicines based on natural sesquiterpene lactones that could effectively modulate TCR responses. Further detailed studies are warranted to define the molecular targets and define the therapeutic potential of these natural sesquiterpene lactones as previously undescribed immunomodulatory and anti-inflammatory agents.

4. Experimental

4.1. Natural compounds

The sesquiterpene lactones (achillin, arglabin, argolide, argracin, 3β-hydroxyarhalin, artesin, artemisinin, estafiatin, grosheimin, grossmisin, leucomisine, parthenolide, and taurin) were isolated as previously described from different plants of the Asteraceae family, as shown in Table I (Adekenov, 2013; Adekenov et al., 2016; Adekenov et al., 1984; Adekenov, 2017; Adekenova et al., 2016; Akyev et al., 1972; Arystan et al., 2009; Rey et al., 1992). The purity of each compound was determined to be > 98% by normalization of the peak areas detected on an automated high-performance liquid chromatography (HPLC) system (Hewlett–Packard Agilent 1100) with a Zorbax SB-C_{18} column (4.6 × 150 mm) eluted with acetonitrile/water (50%/50%, v/v) or methanol/water (50%/50%, v/v) at a flow rate of 0.5 mL/min at 25 °C. The elution was monitored at 204 nm.

4.2. Materials

Dimethyl sulfoxide (DMSO), *N*-formyl-Met-Leu-Phe (*f*MLF), and Histopaque 1077 were purchased from Sigma-Aldrich Chemical Co. (St. Louis, MO, USA). Fluo-4AM dye was from Invitrogen (Carlsbad, CA, USA). NEM was from Chem-Impex International, Inc. (Wood Dale, IL, USA). Anti-human CD3 and anti-human CD28 monoclonal antibodies were purchased from eBioscience (San Diego, CA, USA). Thapsigargin and Trp-Lys-Tyr-Met-Val-Met (WKYMVM) were from Tocris Bioscience (Ellisville, MO, USA). GEE was from Cayman Chemical Co. (Ann Arbor, MI, USA). Ficoll-Paque was from GE Healthcare Bio-Science AB (Uppsala, Sweden). Penicillin–streptomycin solution was purchased from Mediatech (Herndon, VA, USA). Fetal bovine serum (FBS) was purchased from Atlas Biologicals (Fort Collins, CO, USA). Hanks' balanced salt solution (HBSS; 0.137 M NaCl, 5.4 mM KCl, 0.25 mM Na_2HPO_4, 0.44 mM KH_2PO_4, 4.2 mM $NaHCO_3$, 5.56 mM glucose, and 10 mM HEPES, pH 7.4) was from Life Technologies (Grand Island, NY, USA). HBSS

without Ca^{2+} and Mg^{2+} is designated as $HBSS^{-}$; HBSS containing 1.3 mM $CaCl_2$ and 1.0 mM $MgSO_4$ is designated as $HBSS^{+}$. Phosphate buffer solution (PBS, pH 7.2) supplemented with 0.1% sodium azide and 1% bovine serum albumin is referred as flow cytometry buffer (eBioscience).

4.3. Cell culture

Human Jurkat T acute lymphoblastic leukemia cells and human promyelocytic leukemia cells (HL60 cells) stably transfected with FPR1 (FPR1-HL60 cells) or FPR2 (FPR1-HL60 cells) (kind gifts from Dr. Marie-Josephe Rabiet, INSERM, Grenoble, France) were cultured in Roswell Park Memorial Institute (RPMI)-1640 supplemented with 10% heat-inactivated FBS, 10 mM HEPES, 100 μg/mL streptomycin, and 100 U/mL penicillin. Transfected HL60 cells were cultured in the presence of G418 (1 mg/mL). All cell lines were incubated in a humidified incubator at 37 °C with an atmosphere of 5% CO_2.

4.4. Isolation of human neutrophils

For isolation of human neutrophils, blood was collected from healthy donors in accordance with a protocol approved by the Institutional Review Board at Montana State University. Neutrophils were purified from the blood using dextran sedimentation, followed by Ficoll-Paque 1077 gradient separation and hypotonic lysis of red blood cells, as described previously (Schepetkin et al., 2007). Isolated neutrophils were washed twice and resuspended in HBSS. Neutrophil preparations were routinely >95% pure, as determined by light microscopy, and >98% viable, as determined by trypan blue exclusion. Neutrophils were obtained from multiple donors (n=8); however, the cells from different donors were never pooled together during experiments.

4.5. Isolation of human T cells

For isolation of human T cells, blood was collected from healthy donors in accordance with a protocol approved by the Institutional Review Board at Montana State University. Peripheral blood mononuclear cells (PBMCs) were isolated from the blood samples by gradient centrifugation using Ficoll-Paque. $CD3^{+}$ T cells were isolated by negative selection using a pan T cell isolation kit, as described by the manufacturer (Miltnyei Biotec Inc., Auburn, CA) and cultured overnight in RPMI-1640 supplemented with 10% heat-inactivated FBS, 10 mM HEPES, 100 μg/mL streptomycin, and 100 U/mL penicillin. The purified $CD3^{+}$ T cells were used for experiments the following day.

4.6. Protein kinase array

Analysis of the phosphorylation profiles of kinases and their protein substrates was performed using a human phospho-kinase array kit Proteome Profiler (R&D Systems, Minneapolis, MN). The array simultaneously detects 43 kinase phosphorylation sites, including MAPKs [ERK1/2, c-Jun N-terminal kinases (JNK 1–3), and p38α], MSK1/2, mTOR, Akt 1-3, glycogen synthase kinases (GSK-3) α/β, p90 ribosomal S6 kinases (RSK) 1-3, p70 S6 kinase (p70S6K), AMP-activated protein kinase (AMPK) α1 and α2, WNK lysine deficient protein kinase 1 (WNK1), checkpoint kinase 2 (Chk-2), two receptor tyrosine-protein kinases [epidermal growth factor receptor (EGF-R) and platelet-derived

growth factor receptor (PDGF-Rβ)], non-receptor tyrosine-protein kinases (Src, Lyn, Lck, Fyn, Yes, Fgr, Hck, PYK2, FAK/PTK2), cAMP response element-binding protein (CREB), p53, STAT2, STAT3, STAT5a, STAT5b, STAT6, chaperone heat shock protein (hsp) 27, endothelial nitric oxide synthase (eNOS), phospholipase C-γ1 (PLCγ1), cyclin-dependent kinase inhibitor p27 (Kip1), and proline-rich Akt1 substrate 1 (PRAS). For the analysis, Jurkat T cells were incubated for 20 min with the selected compounds or negative control (1% DMSO) at 37 °C, followed by addition of anti-CD3/C28 (10 μg/ml of each antibody) and a 5-min incubation at room temperature. The cells were then lysed, and the arrays were incubated overnight at 4°C with lysates obtained from 10^7 cells for each sample. The arrays were washed three times with 20 ml of the wash buffer and incubated for 2 h with the detection antibody cocktail containing phospho-site-specific biotinylated antibodies. The wash steps were repeated, after which the arrays were exposed to chemiluminescent reagents, and the signal was captured with an Alpha Innotech FluorChem FC2 imaging system.

4.7. Kinase profiling

Kinase profiling was performed by KINOMEscan (DiscoveRx, San Diego, CA, USA) using a panel of 95 protein kinases, as described previously (Fabian et al., 2005). In brief, kinases were produced and displayed on T7 phage or expressed in HEK-293 cells. Binding reactions were performed at room temperature for 1 h, and the fraction of kinase not bound to test compound was determined by capture with an immobilized affinity ligand and quantified by quantitative polymerase chain reaction. Primary screening at fixed concentration (10 μM) of a test compound was performed in duplicate.

4.8. ERK1/2 enzyme-linked immunosorbent assay (ELISA)

Jurkat T cells or isolated human T cells were incubated for 20 min with the selected compounds or negative control (1% DMSO) at 37 °C, followed by addition of either anti-CD3/C28 monoclonal antibodies (10 μg/ml of each antibody) for Jurkat T cells or Dynabead human T-activator CD3/CD28 beads for primary T cells (bead-to-cell ratio 1:1) and a 5-min incubation at room temperature. The cells were lysed with a lysis buffer (R&D Systems), and the levels of phosphorylated ERK1/2 were measured in the cell lysates using an ELISA kit (R&D Systems) for human phospho-ERK1 (Thr202/Tyr204)/ERK2 (Thr185/Tyr187). The concentrations of phospho-ERK1/2 in the cell lysates were determined using a calibration curve with recombinant human phosphor-ERK2 (Thr85/Tyr187).

4.9. Ca^{2+} mobilization assay

Changes in intracellular Ca^{2+} concentrations ($[Ca^{2+}]_i$) were measured with a FlexStation 3 scanning fluorometer (Molecular Devices, Sunnyvale, CA, USA). Briefly, cells (human neutrophils, HL60 cells or Jurkat cells) were suspended in HBSS, loaded with Fluo-4AM (Invitrogen, Carlsbad, CA, USA) at a final concentration of 1.25 μg/mL and incubated for 30 min in the dark at 37 °C. After dye loading, the cells were washed with $HBSS^-$, resuspended in $HBSS^+$, separated into aliquots, and aliquoted into the wells of flat-bottom, half-area well black microtiter plates (2×10^5 cells/well). Test compounds diluted in DMSO were added to the wells (final concentration of DMSO was 1%), and changes in fluorescence were monitored (λ_{ex} = 485 nm, λ_{em} = 538 nm) every 5 s for 240 s at room temperature after

addition of test compounds to evaluate direct agonist effects. To evaluate inhibitory effects, Jurkat T cells were pretreated for 20 min with various concentrations of test compound, followed by addition of 10 μg/ml anti-CD3 antibody. The maximum change in fluorescence, expressed in arbitrary units over baseline, was used to determine the agonist response. Responses were normalized to the response induced by anti-CD3 for Jurkat cells, 5 nM *f*MLF (neutrophils and FPR1 HL60 cells), or 5 nM WKYMVM (FPR2 HL60 cells) which was assigned a value of 100%. Curve fitting (at least five or six points) and calculation of median effective concentration values (IC_{50}) were performed by nonlinear regression analysis of the dose–response curves generated using Prism 7 (GraphPad Software, Inc., San Diego, CA, USA).

4.10. Flow cytometry

Jurkat T cells (1×10^6 cells) were incubated in 100 μl $HBSS^+$ containing different concentrations of test sesquiterpene lactones or anti-human CD3 monoclonal antibody for 20 min at 37 °C. The cells were next stained with 1.25 μg/ml of allophycocyanin (APC)-conjugated anti-human CD3 (Affymetrix eBioscience, San Diego, CA, USA) or 5 μg/ml of APC-conjugated mouse IgG_1 isotype control (Affymetrix eBioscience) for 30 min on ice. The cells were then washed, resuspended in flow cytometry buffer, and analyzed using an LSR II flow cytometer (Becton Dickinson, Sunnyvale, CA, USA) with FAXDiva Software, v.8.0.1.

4.11. Assessment of compound cytotoxicity

Cytotoxicity was analyzed with a CellTiter-Glo Luminescent Cell Viability Assay Kit (Promega, Madison, WI, USA). Briefly, Jurkat T cells or isolated human T cells were cultured at a density of 2×10^5 cells/well with different concentrations of compound under investigation for 30 min at 37 °C. Following treatment, substrate was added, and the samples were analyzed with a Fluoroscan Ascent FL microplate reader.

4.12. Glutathione (GSH) assay

Jurkat cells were plated at 10,000 cells per well in white 96-well half-area plates. After addition of test sesquiterpene lactones or vehicle (1% DMSO) negative control, the cells were incubated for 30 min at 37 °C, and total GSH was measured using a GSHGlo™ assay (Promega Corp., Madison, WI, USA), according to manufacturer's instructions (Harling et al., 2013). Luminescence was measured with a Fluroscan Ascent FL microplate reader (Thermo Electron, Waltham, MA).

Acknowledgments

This research was supported in part by National Institutes of Health IDeA Program COBRE Grant GM110732; USDA National Institute of Food and Agriculture Hatch project 1009546; Montana University System Research Initiative: 51040-MUSRI2015-03; and the Montana State University Agricultural Experiment Station.

Abbreviations used

DMSO	dimethyl sulfoxide
FBS	fetal bovine serum

FPR	*N*-formyl peptide receptor
HBSS	Hanks' balanced salt solution
IP3	inositol triphosphate
ITAM	immune-receptor tyrosine-based activation motif
TCR	T cell receptor
ERK	extracellular signal-regulated kinase
MAPK	mitogen-activated protein kinases
SERCA	sarco/endoplasmic reticulum Ca^{2+} ATPase
GEE	glutathione ethylene ester
GSH	glutathione
ELISA	enzyme-linked immunosorbent assay
PLC	phospholipase C

References

Adekenov SM. Sesquiterpene lactones from endemic species of the family Asteraceae. Chem Nat Compd. 2013; 1:158–162.

Adekenov SM. Chemical modification of arglabin and biological activity of its new derivatives. Fitoterapia. 2016; 110:196–205. [PubMed: 26625839]

Adekenov SM, Makubaeva AI, Kokkozov DN, Kanafin EN, Korneev VS, Gatilov YV, Kishkentaeva AS, Atazhanova GA. Chemical Composition of Artemisia aralensis. Chem Nat Compd. 2016; 52:417–420.

Adekenov SM, Muchametzhanov MN, Kagarlitskii AD, Turmuchambetov AZ. Chemical Investigation of Achillea-Nobilis. Khim Prir Soedin+. 1984:603–607.

Adekenov SM, Shaimerdenova ZR, Gatilov YuV, Atazhanova GA. Two new sesquiterpene lactones from Arthemisia halophile. Chem Nat Compd. 2017; 53:241–245.

Adekenova AS, Sakenova PY, Ivasenko SA, Khabarov IA, Adekenov SM, Berthod A. Gram-Scale Purification of Two Sesquiterpene Lactones from Chartolepsis Intermedia Boiss. Chromatographia. 2016; 79:37–43.

Akyev B, Kasymov SZ, Sidyakin GP. Artesin - New Sesquiterpenic Lactone from Artemisia-Santolina. Khim Prir Soedin+. 1972:733–735.

Arystan LI, Adekenov SM, Itzhanova Kh I, Sariev AK. Effect of leucomisine on cell and humoral immunity indices. Eksp Klin Farmakol. 2009; 72:30–32. [PubMed: 20095397]

Butturini E, de Prati AC, Chiavegato G, Rigo A, Cavalieri E, Darra E, Mariotto S. Mild oxidative stress induces S-glutathionylation of STAT3 and enhances chemosensitivity of tumoural cells to chemotherapeutic drugs. Free Radic Biol Med. 2013; 65:1322–1330. [PubMed: 24095958]

Carlisi D, Buttitta G, Di Fiore R, Scerri C, Drago-Ferrante R, Vento R, Tesoriere G. Parthenolide and DMAPT exert cytotoxic effects on breast cancer stem-like cells by inducing oxidative stress, mitochondrial dysfunction and necrosis. Cell Death Dis. 2016; 7:e2194. [PubMed: 27077810]

Cattaneo F, Parisi M, Ammendola R. Distinct signaling cascades elicited by different formyl Peptide receptor 2 (FPR2) agonists. Int J Mol Sci. 2013; 14:7193–7230. [PubMed: 23549262]

Cerveira J, Begum J, Di Marco Barros R, van der Veen AG, Filby A. An imaging flow cytometry-based approach to measuring the spatiotemporal calcium mobilisation in activated T cells. J Immunol Methods. 2015; 423:120–130. [PubMed: 25967946]

Chadwick M, Trewin H, Gawthrop F, Wagstaff C. Sesquiterpenoids lactones: benefits to plants and people. Int J Mol Sci. 2013; 14:12780–12805. [PubMed: 23783276]

D'Anneo A, Carlisi D, Lauricella M, Emanuele S, Di Fiore R, Vento R, Tesoriere G. Parthenolide induces caspase-independent and AIF-mediated cell death in human osteosarcoma and melanoma cells. J Cell Physiol. 2013; 228:952–967. [PubMed: 22688575]

Davis W Jr, Ronai Z, Tew KD. Cellular thiols and reactive oxygen species in drug-induced apoptosis. J Pharmacol Exp Ther. 2001; 296:1–6. [PubMed: 11123355]

Eckstein-Ludwig U, Webb RJ, Van Goethem IDA, East JM, Lee AG, Kimura M, O'Neill PM, Bray PG, Ward SA, Krishna S. Artemisinins target the SERCA of Plasmodium falciparum. Nature. 2003; 424:957–961. [PubMed: 12931192]

Engreitz JM, Daigle BJ Jr, Marshall JJ, Altman RB. Independent component analysis: mining microarray data for fundamental human gene expression modules. J Biomed Inf. 2010; 43:932–944.

Fabian MA, Biggs WH III, Treiber DK, Atteridge CE, Azimioara MD, Benedetti MG, Carter TA, Ciceri P, Edeen PT, Floyd M, Ford JM, Galvin M, Gerlach JL, Grotzfeld RM, Herrgard S, Insko DE, Insko MA, Lai AG, Lelias JM, Mehta SA, Milanov ZV, Velasco AM, Wodicka LM, Patel HK, Zarrinkar PP, Lockhart DJ. A small molecule-kinase interaction map for clinical kinase inhibitors. Nat Biotechnol. 2005; 23:329–336. [PubMed: 15711537]

Fu G, Chen Y, Yu M, Podd A, Schuman J, He Y, Di L, Yassai M, Haribhai D, North PE, Gorski J, Williams CB, Wang D, Wen R. Phospholipase Cγ1 is essential for T cell development, activation, and tolerance. J Exp Med. 2010; 207:309–318. [PubMed: 20123962]

Garcia-Pineres AJ, Castro V, Mora G, Schmidt TJ, Strunck E, Pahl HL, Merfort I. Cysteine 38 in p65/NF-κB plays a crucial role in DNA binding inhibition by sesquiterpene lactones. J Biol Chem. 2001; 276:39713–39720. [PubMed: 11500489]

Garcia-Pineres AJ, Lindenmeyer MT, Merfort I. Role of cysteine residues of p65/NF-kappaB on the inhibition by the sesquiterpene lactone parthenolide and N-ethyl maleimide, and on its transactivating potential. Life Sci. 2004; 75:841–856. [PubMed: 15183076]

Gringhuis SI, Papendrecht-van der Voort EA, Leow A, Nivine Levarht EW, Breedveld FC, Verweij CL. Effect of redox balance alterations on cellular localization of LAT and downstream T-cell receptor signaling pathways. Mol Cell Biol. 2002; 22:400–411. [PubMed: 11756537]

Gripentrog JM, Miettinen HM. Formyl peptide receptor-mediated ERK1/2 activation occurs through G(i) and is not dependent on beta-arrestin1/2. Cell Signal. 2008; 20:424–431. [PubMed: 18060741]

Harling JD, Deakin AM, Campos S, Grimley R, Chaudry L, Nye C, Polyakova O, Bessant CM, Barton N, Somers D, Barrett J, Graves RH, Hanns L, Kerr WJ, Solari R. Discovery of novel irreversible inhibitors of interleukin (IL)-2-inducible tyrosine kinase (Itk) by targeting cysteine 442 in the ATP pocket. J Biol Chem. 2013; 288:28195–28206. [PubMed: 23935099]

Heller M, Watts JD, Aebersold R. CD28 stimulation regulates its association with N-ethylmaleimide-sensitive fusion protein and other proteins involved in vesicle sorting. Proteomics. 2001; 1:70–78. [PubMed: 11680900]

Heppner DE, Hristova M, Dustin CM, Danyal K, Habibovic A, van der Vliet A. The NADPH Oxidases DUOX1 and NOX2 Play Distinct Roles in Redox Regulation of Epidermal Growth Factor Receptor Signaling. J Biol Chem. 2016; 291:23282–23293. [PubMed: 27650496]

Hou L, Huang H. Immune suppressive properties of artemisinin family drugs. Pharmacol Ther. 2016; 166:123–127. [PubMed: 27411673]

Hsu MF, Sun SP, Chen YS, Tsai CR, Huang LJ, Tsao LT, Kuo SC, Wang JP. Distinct effects of N-ethylmaleimide on formyl peptide- and cyclopiazonic acid-induced Ca2+ signals through thiol modification in neutrophils. Biochem Pharmacol. 2005; 70:1320–1329. [PubMed: 16143313]

Huang C, Ba Q, Yue Q, Li J, Li J, Chu R, Wang H. Artemisinin rewires the protein interaction network in cancer cells: network analysis, pathway identification, and target prediction. Mol Biosyst. 2013; 9:3091–3100. [PubMed: 24085322]

Ishikawa J, Ohga K, Yoshino T, Takezawa R, Ichikawa A, Kubota H, Yamada T. A pyrazole derivative, YM-58483, potently inhibits store-operated sustained Ca2+ influx and IL-2 production in T lymphocytes. J Immunol. 2003; 170:4441–4449. [PubMed: 12707319]

Itoh T, Ohguchi K, Nozawa Y, Akao Y. Intracellular glutathione regulates sesquiterpene lactone-induced conversion of autophagy to apoptosis in human leukemia HL60 cells. Anticancer Res. 2009; 29:1449–1457. [PubMed: 19414401]

Johnston PA, Shinde SN, Hua Y, Shun TY, Lazo JS, Day BW. Development and validation of a high-content screening assay to identify inhibitors of cytoplasmic dynein-mediated transport of glucocorticoid receptor to the nucleus. Assay Drug Dev Technol. 2012; 10:432–456. [PubMed: 22830992]

Kim JE, White FM. Quantitative analysis of phosphotyrosine signaling networks triggered by CD3 and CD28 costimulation in Jurkat cells. J Immunol. 2006; 176:2833–2843. [PubMed: 16493040]

Kim JY, Cheon YH, Yoon KH, Lee MS, Oh J. Parthenolide inhibits osteoclast differentiation and bone resorbing activity by down-regulation of NFATc1 induction and c-Fos stability, during RANKL-mediated osteoclastogenesis. BMB Rep. 2014; 47:451–456. [PubMed: 24314143]

Koike T, Yamagishi H, Hatanaka Y, Fukushima A, Chang JW, Xia Y, Fields M, Chandler P, Iwashima M. A novel ERK-dependent signaling process that regulates interleukin-2 expression in a late phase of T cell activation. J Biol Chem. 2003; 278:15685–15692. [PubMed: 12595531]

Kuo LM, Kuo CY, Lin CY, Hung MF, Shen JJ, Hwang TL. Intracellular glutathione depletion by oridonin leads to apoptosis in hepatic stellate cells. Molecules. 2014; 19:3327–3344. [PubMed: 24647034]

Lagoutte R, Serba C, Abegg D, Hoch DG, Adibekian A, Winssinger N. Divergent synthesis and identification of the cellular targets of deoxyelephantopins. Nature Communications. 2016:7.

Lane TA, Lamkin GE. Phagocytosis-induced chemotaxis receptor cycling in neutrophils is mediated by thiol oxidation. Blood. 1982; 59:1337–1343. [PubMed: 6282363]

Larghi P, Williamson DJ, Carpier JM, Dogniaux S, Chemin K, Bohineust A, Danglot L, Gaus K, Galli T, Hivroz C. VAMP7 controls T cell activation by regulating the recruitment and phosphorylation of vesicular Lat at TCR-activation sites. Nat Immunol. 2013; 14:723–731. [PubMed: 23666293]

Li-Weber M, Giaisi M, Treiber MK, Krammer PH. The anti-inflammatory sesquiterpene lactone parthenolide suppresses IL-4 gene expression in peripheral blood T. Eur J Immunol. 2002; 32:3587–3597. [PubMed: 12516545]

Liu Y, Huang X, Li Y, Li C, Hu X, Xue C, Meng F, Zhou P. Ursolic acid promotes robust tolerance to cardiac allografts in mice. Clin Exp Immunol. 2011; 164:282–288. [PubMed: 21391985]

Lovatt M, Filby A, Parravicini V, Werlen G, Palmer E, Zamoyska R. Lck regulates the threshold of activation in primary T cells, while both Lck and Fyn contribute to the magnitude of the extracellular signal-related kinase response. Mol Cell Biol. 2006; 26:8655–8665. [PubMed: 16966372]

Mak TW, Grusdat M, Duncan GS, Dostert C, Nonnenmacher Y, Cox M, Binsfeld C, Hao Z, Brustle A, Itsumi M, Jager C, Chen Y, Pinkenburg O, Camara B, Ollert M, Bindslev-Jensen C, Vasiliou V, Gorrini C, Lang PA, Lohoff M, Harris IS, Hiller K, Brenner D. Glutathione primes t cell metabolism for inflammation. Immunity. 2017; 46:675–689. [PubMed: 28423341]

Miyata N, Gon Y, Nunomura S, Endo D, Yamashita K, Matsumoto K, Hashimoto S, Ra C. Inhibitory effects of parthenolide on antigen-induced microtubule formation and degranulation in mast cells. Int Immunopharmacol. 2008; 8:874–880. [PubMed: 18442792]

Philipsen L, Engels T, Schilling K, Gurbiel S, Fischer KD, Tedford K, Schraven B, Gunzer M, Reichardt P. Multimolecular analysis of stable immunological synapses reveals sustained recruitment and sequential assembly of signaling clusters. Mol Cell Proteomics. 2013; 12:2551–2567. [PubMed: 23754785]

Ploger M, Sendker J, Langer K, Schmidt TJ. Covalent modification of human serum albumin by the natural sesquiterpene lactone parthenolide. Molecules. 2015; 20:6211–6223. [PubMed: 25859779]

Reddie KG, Carroll KS. Expanding the functional diversity of proteins through cysteine oxidation. Curr Opin Chem Biol. 2008; 12:746–754. [PubMed: 18804173]

Ren Y, Yu J, Kinghorn AD. Development of anticancer agents from plant-derived sesquiterpene lactones. Curr Med Chem. 2016; 23:2397–2420. [PubMed: 27160533]

Rey JP, Levesque J, Pousset JL. Extraction and High-Performance Liquid-Chromatographic Methods for the Gamma-Lactones Parthenolide (Chrysanthemum Parthenium Bernh), Marrubiin (Marrubium-Vulgare L) and Artemisinin (Artemisia-Annua L). J Chromatogr. 1992; 605:124–128.

Rogers TB, Inesi G, Wade R, Lederer WJ. Use of thapsigargin to study Ca^{2+} homeostasis in cardiac cells. Biosci Rep. 1995; 15:341–349. [PubMed: 8825036]

Saadane A, Eastman J, Berger M, Bonfield TL. Parthenolide inhibits ERK and AP-1 which are dysregulated and contribute to excessive IL-8 expression and secretion in cystic fibrosis cells. J Inflamm. 2011; 8:26.

Sauer EL, Cloake NC, Greer JM. Taming the TCR: antigen-specific immunotherapeutic agents for autoimmune diseases. Int Rev Immunol. 2015; 34:460–485. [PubMed: 25970132]

Scarponi C, Butturini E, Sestito R, Madonna S, Cavani A, Mariotto S, Albanesi C. Inhibition of inflammatory and proliferative responses of human keratinocytes exposed to the sesquiterpene lactones dehydrocostuslactone and costunolide. PLoS One. 2014; 9:e107904. [PubMed: 25226283]

Schepetkin IA, Kirpotina LN, Khlebnikov AI, Cheng N, Ye RD, Quinn MT. Antagonism of human formyl peptide receptor 1 (FPR1) by chromones and related isoflavones. Biochem Pharmacol. 2014; 92:627–641. [PubMed: 25450672]

Schepetkin IA, Kirpotina LN, Khlebnikov AI, Quinn MT. High-throughput screening for small-molecule activators of neutrophils: Identification of novel N-formyl peptide receptor agonists. Mol Pharmacol. 2007; 71:1061–1074. [PubMed: 17229869]

Tew KD, Townsend DM. Regulatory functions of glutathione S-transferase P1-1 unrelated to detoxification. Drug Metab Rev. 2011; 43:179–193. [PubMed: 21351850]

Visperas PR, Wilson CG, Winger JA, Yan Q, Lin K, Arkin MR, Weiss A, Kuriyan J. Identification of inhibitors of the association of ZAP-70 with the t cell receptor by high-throughput screen. SLAS Discov. 2017; 22:324–331. [PubMed: 27932698]

Visperas PR, Winger JA, Horton TM, Shah NH, Aum DJ, Tao A, Barros T, Yan QR, Wilson CG, Arkin MR, Weiss A, Kuriyan J. Modification by covalent reaction or oxidation of cysteine residues in the tandem-SH2 domains of ZAP-70 and Syk can block phosphopeptide binding. Biochem J. 2015; 465:149–161. [PubMed: 25287889]

Wagner S, Hofmann A, Siedle B, Terfloth L, Merfort I, Gasteiger J. Development of a structural model for NF-κB inhibition of sesquiterpene lactones using self-organizing neural networks. J Med Chem. 2006; 49:2241–2252. [PubMed: 16570920]

Wang JX, Tang W, Yang ZS, Wan J, Shi LP, Zhang Y, Zhou R, Ni J, Hou LF, Zhou Y, He PL, Yang YF, Li Y, Zuo JP. Suppressive effect of a novel water-soluble artemisinin derivative SM905 on T cell activation and proliferation in vitro and in vivo. Eur J Pharmacol. 2007; 564:211–218. [PubMed: 17349993]

Wang Y, Huang ZQ, Wang CQ, Wang LS, Meng S, Zhang YC, Chen T, Fan YQ. Artemisinin inhibits extracellular matrix metalloproteinase inducer (EMMPRIN) and matrix metalloproteinase-9 expression via a protein kinase Cδ/p38/extracellular signal-regulated kinase pathway in phorbol myristate acetate-induced THP-1 macrophages. Clin Exp Pharmacol Physiol. 2011; 38:11–18. [PubMed: 21039753]

Whipple RA, Vitolo MI, Boggs AE, Charpentier MS, Thompson K, Martin SS. Parthenolide and costunolide reduce microtentacles and tumor cell attachment by selectively targeting detyrosinated tubulin independent from NF-κB inhibition. Breast Cancer Res. 2013:15.

Winslow MM, Neilson JR, Crabtree GR. Calcium signalling in lymphocytes. Curr Opin Immunol. 2003; 15:299–307. [PubMed: 12787755]

Xu CQ, Call ME, Wucherpfennig KW. A membrane-proximal tetracysteine motif contributes to assembly of CD3δε and CD3γε dimers with the T cell receptor. J Biol Chem. 2006; 281:36977–36984. [PubMed: 17023417]

Ye Y, Chao XJ, Wu JF, Cheng BCY, Su T, Fu XQ, Li T, Guo H, Tse AKW, Kwan HY, Du J, Chou GX, Yu ZL. ERK/GSK3β signaling is involved in atractylenolide I-induced apoptosis and cell cycle arrest in melanoma cells. Oncol Rep. 2015; 34:1543–1548. [PubMed: 26151480]

Zhang HH, Kuang S, Wang Y, Sun XX, Gu Y, Hu LH, Yu Q. Bigelovin inhibits STAT3 signaling by inactivating JAK2 and induces apoptosis in human cancer cells. Acta Pharmacol Sin. 2015; 36:507–516. [PubMed: 25619393]

Zhang W, Sloan-Lancaster J, Kitchen J, Trible RP, Samelson LE. LAT: the ZAP-70 tyrosine kinase substrate that links T cell receptor to cellular activation. Cell. 1998; 92:83–92. [PubMed: 9489702]

Highlights

1. Thirteen natural sesquiterpene lactones were evaluated for their ability to inhibit inflammatory T cell responses.
2. Five natural sesquiterpene lactones inhibited early steps in T cell activation, including several kinases.
3. The active natural sesquiterpene lactones also depleted T cell intracellular glutathione levels.
4. The ability to inhibit initial phases of TCR activation suggests these natural compounds may have novel immunotherapeutic properties.

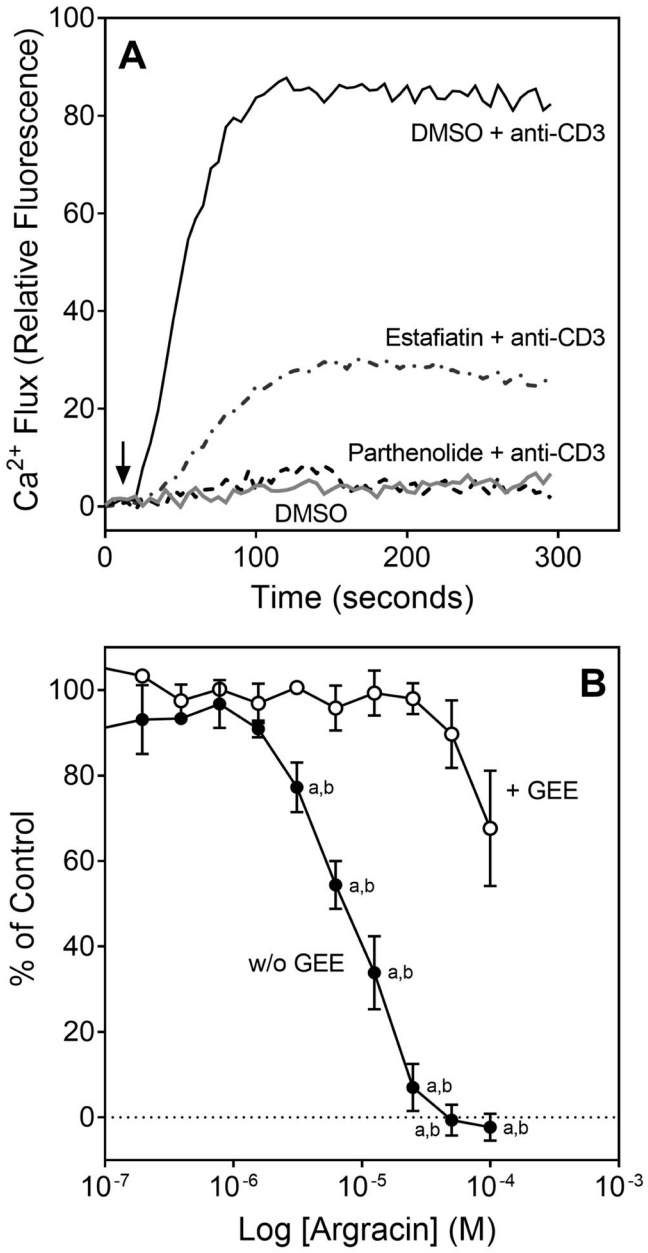

Figure 1.

Effect of parthenolide, estafiatin, and agracin on activation-induced Ca^{2+} mobilization in Jurkat T cells. **Panel A**. Jurkat cells were pretreated for 20 min with 1% DMSO (negative control), estafiatin (50 μM), or parthenolide (50 μM), and the kinetics of Ca^{2+} mobilization 15 sec after activation with 5 μg/ml anti-CD3 monoclonal antibody were measured (arrow indicates time of activation). The response of control cells treated with DMSO alone is shown as a grey line. **Panel B**. Jurkat cells were pretreated for 3 h with 5 mM GEE (+ GEE) or medium (w/o GEE), followed by treatment for 20 min with control 1% DMSO or increasing concentrations of argracin and activated with anti-CD3. Activation-induced Ca^{2+} flux was measured as described, and the results are shown as % of maximal activation

measured in control cells. The results shown in both panels are representative of three independent experiments. Statistically significant differences between cells pretreated with argracin versus control (1% DMSO) are indicated ($^{a}p<0.01$). In addition, statistically significant differences between cells incubated with GEE versus without GEE prior to the argracin treatment and activation are indicated ($^{b}p<0.01$).

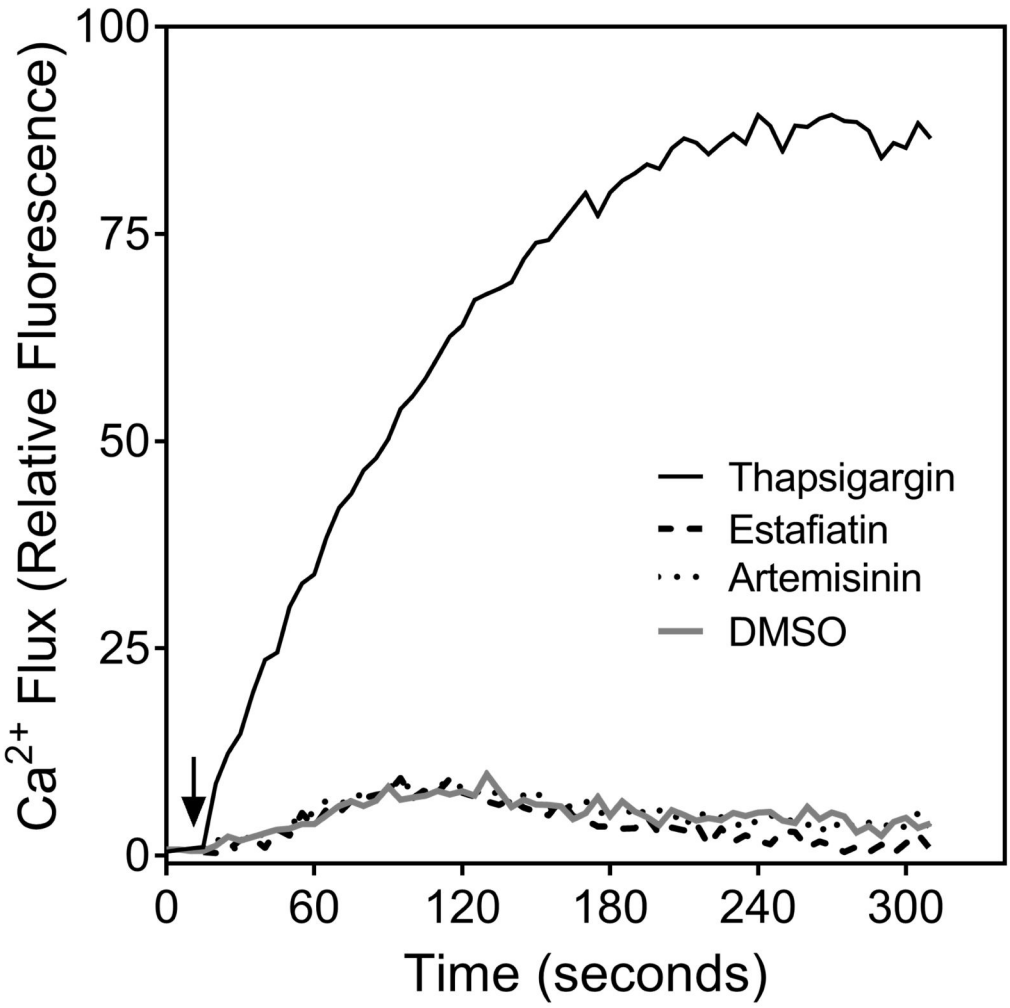

Figure 2.

Effect of thapsigargin, estafiatin, and artemisinin on Ca^{2+} mobilization in Jurkat T cells. Jurkat cells were treated with 1% DMSO (negative control), 200 nM thapsigargin, 50 μM estafiatin, or 50 μM artemisinin, as indicated, and the kinetics of Ca^{2+} mobilization were measured (arrow indicates time of compound addition). The results shown are representative of three independent experiments.

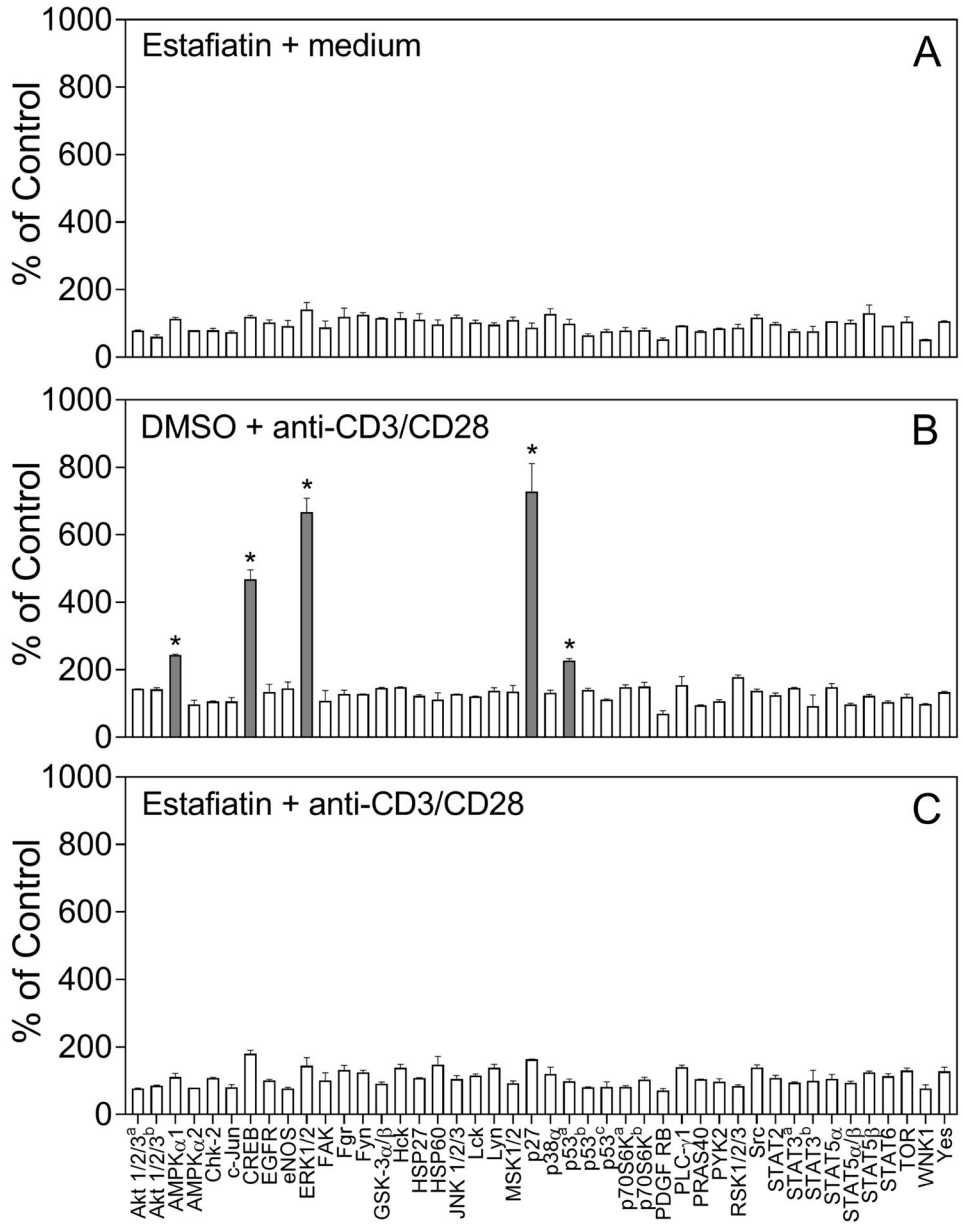

Figure 3.

Effect of estafiatin on activation-induced kinase phosphorylation in Jurkat T cells. Jurkat T cells were pretreated for 20 min with estafiatin (50 μM), followed by activation with anti-CD3/CD28 (10 μg/ml each) for 5 min, and the levels of protein phosphorylation in cell lysates were evaluated using a human phospho-kinase array. There are several kinases with different phosphorylation sites, including Akt1/2/3[a] on Ser473 and Akt1/2/3[b] on Thr303; p70S6K[a] on Thr389 and p70S6K[b] on Thr421/S424; STAT3[a] on Tyr705 and STAT3[b] on Ser727; p53[a], p53[b], and p53[c], on Ser392, Ser46, and Ser15, respectively. The data are presented as mean ± SD of duplicate samples. Statistically significant differences (* $p<0.05$) between DMSO (control) and estafiatin-pretreated cells are indicated (also shown in shaded bars).

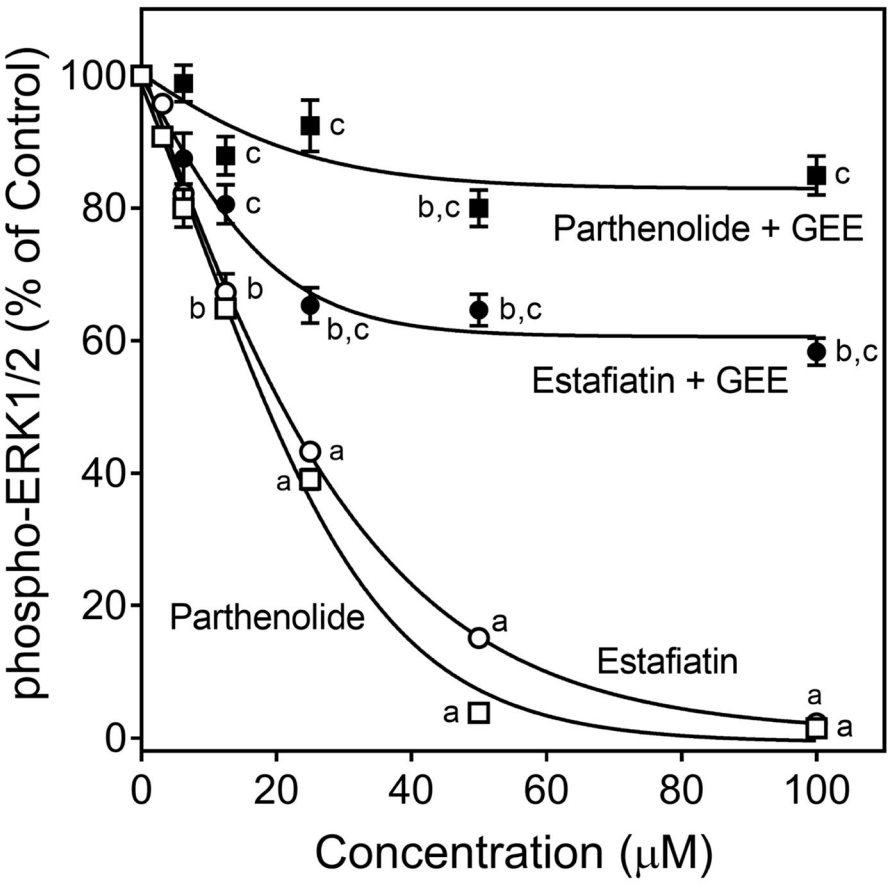

Figure 4.

Effect of parthenolide and estafiatin on activation-induced ERK1/2 phosphorylation. Jurkat T cells were pretreated with 1% DMSO or increasing concentrations of estafiatin (○) or parthenolide (□) for 20 min, followed by activation with anti-CD3/CD28 (10 μg/ml each) for 5 min, and the levels of ERK1/2 phosphorylation were evaluated using ELISA. In some experiments, Jurkat cells were incubated overnight with 2 mM GEE or medium (not shown), followed by treatment with DMSO or increasing concentrations of estafiatin (●) or parthenolide (■) for 20 min, followed by activation with anti-CD3/CD28 (10 μg/ml each) for 5 min, and ERK1/2 phophorylation was evaluated using the same procedures described above. The data are presented as % of control levels and represent the mean ± SD of triplicate samples from one experiment, which is representative of three independent experiments. Statistically significant differences between cells pretreated with sesquiterpene lactones versus control (1% DMSO) are indicated ($^{a}p<0.01$; $^{b}p<0.05$). In addition, statistically significant differences between cells incubated with GEE versus without GEE prior to the respective lactone treatment and activation are indicated ($^{c}p<0.01$).

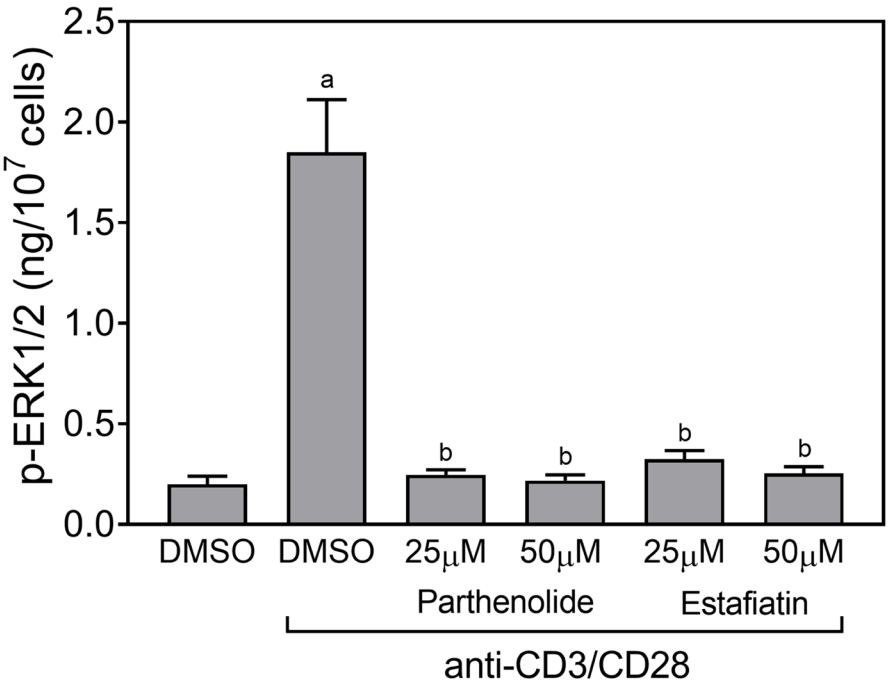

Figure 5.

Effect of parthenolide and estafiatin on activation-induced ERK1/2 phosphorylation in human primary T cells. Isolated human T cells were pretreated for 20 min with 1% DMSO or the indicated concentrations of parthenolide and estafiatin, followed by activation with human T-activator CD3/CD28 Dynabeads (bead-to-cell ratio 1:1) for 5 min, and the levels of ERK phosphorylation were evaluated using an ELISA for human phospho-ERK1/2. The data are presented as mean ± SD of triplicate samples. Statistically significant differences between cells treated with control DMSO versus DMSO + CD3/CD20 beads ($^{a}p<0.01$) and between cells treated with DMSO + CD3/CD20 beads versus cells treated with the indicated lactones + CD3/CD20 beads ($^{b}p<0.01$) are indicated. The results shown are representative of three independent experiments.

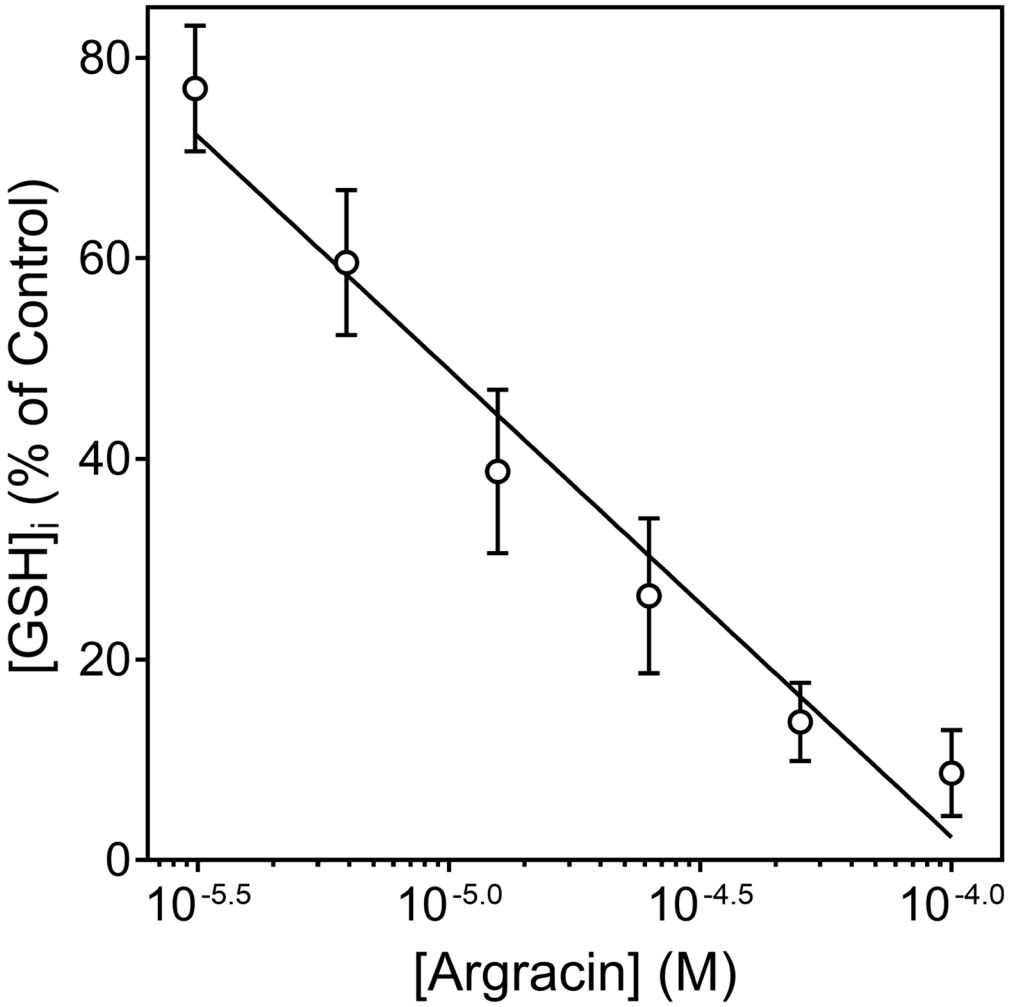

Figure 6.

Effect of agracin on Jurkat T cell cytosolic GSH. Jurkat cells (10^5 cells/ml) were incubated with control 1% DMSO or increasing concentrations of agracin for 20 min at room temperature, and the level of cytosolic $[GSH]_i$ in the cells was measured using a GSHGlo assay. The results are presented as % of $[GSH]_i$ measured in control DMSO treated cells (mean ± SD of triplicate samples) and are representative of three independent experiments.

Table 1

Chemical structures and plant sources of the selected sesquiterpene lactones

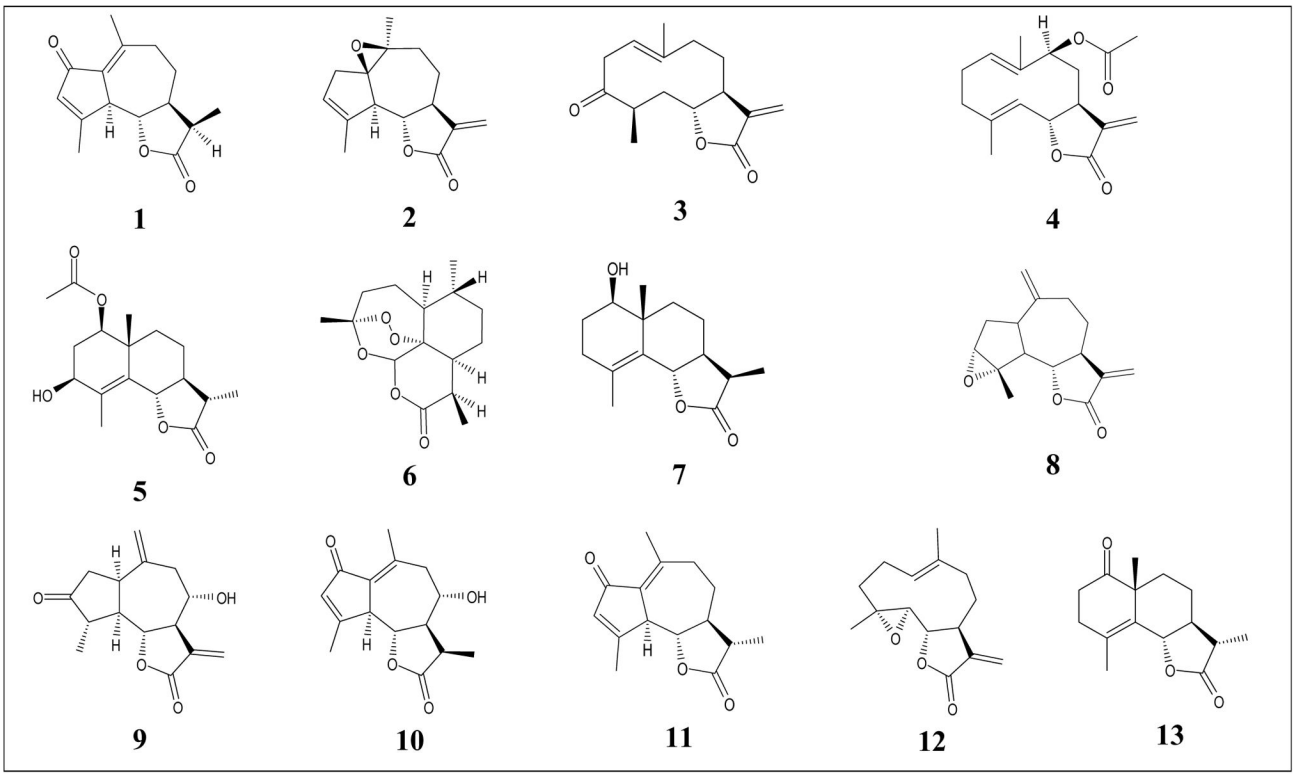

Achillin (**1**), argolide (**3**), and grossmisin (**10**) were isolated from *Artemisia radicans* A. Kuprijanov sp. Nova (Adekenov, 2013); arglabin (**2**) was isolated from *Artemisia filatovae* A. Kuprijanov sp. Nova (Adekenov, 2013); argracin (**4**) was isolated from *Artemisia aralensis* Krasch. (Adekenov et al., 2016); 3β-hydroxyarhalin (**5**) was isolated from *Artemisia halophil3* Krasch. (Adekenov, 2017); artemisinin (**6**) was isolated from *Artemisia annua* L. (Rey et al., 1992); artesin (**7**) and taurin (**13**) were isolated from *Artemisia semiarida* (Krasch. et Lavr.) Filat. (Adekenov, 2013; Akyev et al., 1972); estafiatin (**8**) was isolated from *Achillea nobilis* L. (Adekenov et al., 1984); grosheimin (**9**) was isolated from *Chartolepsis intermedia* Boiss (Adekenova et al., 2016); leucomisine (**11**) was isolated from *Artemisia leucodes* Schrenk (Arystan et al., 2009); and parthenolide (**12**) was isolated from *Tanacetum scopulorum* (Krasch.) Tzvel (Adekenov, 2013).

Table 2

Effect of sesquiterpene lactones on Ca^{2+} mobilization, ERK1/2 phosphorylation, and GSH concentration

Compd.	Name	Jurkat T cells	FPR2-HL60	Jurkat T Cells	FPR1-HL60	FPR2-HL60	PMN	Jurkat T Cells
		p-ERK1/2		Ca^{2+} mobilization				$[GSH]_i$
		IC_{50} (μM)						
1	achillin	N.A.	N.A.	N.A.	N.A.	N.A.	N.A.	N.A.
2	arglabin	28.7 ± 6.3	N.A.	11.1 ± 2.7	N.A.	N.A.	N.A.	18.0 ± 1.8
3	argolide	N.A.	N.A.	N.A.	N.A.	N.A.	N.A.	N.A.
4	argracin	16.8 ± 5.3	N.A.	6.1 ± 1.6	N.A.	N.A.	N.A.	8.9 ± 1.4
5	3β-hydroxyarhalin	N.A.	N.A.	N.A.	N.A.	N.A.	N.A.	N.A.
6	artemisinin	N.A.	N.A.	N.A.	N.A.	N.A.	N.A.	N.A.
7	artesin	N.A.	N.A.	N.A.	N.A.	N.A.	N.A.	N.A.
8	estafiatin	15.4 ± 3.2	N.A.	29.3 ± 6.8	N.A.	N.A.	N.A.	46.9 ± 5.3
9	grosheimin	43.0 ± 7.5	N.A.	15.4 ± 4.3	N.A.	N.A.	N.A.	16.6 ± 4.8
10	grossmisin	N.A.	N.A.	N.A.	N.A.	N.A.	N.A.	N.A.
11	leucomisine	N.A.	N.A.	N.A.	N.A.	N.A.	N.A.	N.A.
12	parthenolide	13.8 ± 1.7	N.A.	2.4 ± 0.6	N.A.	N.A.	N.A.	9.9 ± 3.4
13	taurin	N.A.	N.A.	N.A.	N.A.	N.A.	N.A.	N.A.

Inhibition was evaluated after 20 min pretreatment with test compounds at room temperature, followed by addition of 10 μg/ml anti-CD3/CD28 (p-ERK1/2 in Jurkat cells), 10 μg/ml anti-CD3 (Ca^{2+} flux in Jurkat cells), 5 nM *f*MLF [Ca^{2+} flux in FPR1-HL60 cells and human neutrophils (PMN)], or 5 nM WKYMVM (pERK1/2 and Ca^{2+} flux in FPR2-HL60 cells). Changes in Jurkat T cell cytosolic $[GSH]_i$ were measured after treating cells with test compounds for 30 min at 37°C. N.A., no activity was observed at the highest tested concentration (50 μM in the p-ERK1/2 assay and 100 μM in the GSH assay).